Method for the Acceleration of Transmission-Line Coupling Calculations

Bart Van Thielen and Guy A. E. Vandenbosch, *Member, IEEE*

***Abstract*—In this paper, a fast method for the calculation of mutual coupling between transmission lines is described. Starting from the general method of moments, which can handle random shapes, the calculations are speeded up for the specific case of coupling between lines. This is accomplished by assuming that all lines are terminated in their characteristic impedance and using the traveling current waves on these matched lines. Only first-order coupling between the lines is taken into account. This means that only the current induced by the source line is taken into account and all currents resulting from induction by this induced current are discarded. This results in a much faster method because only the inverse of the Z-matrix for the observation line is involved.**

***Index Terms*—Electromagnetic compatibility, line coupling, method of moments.**

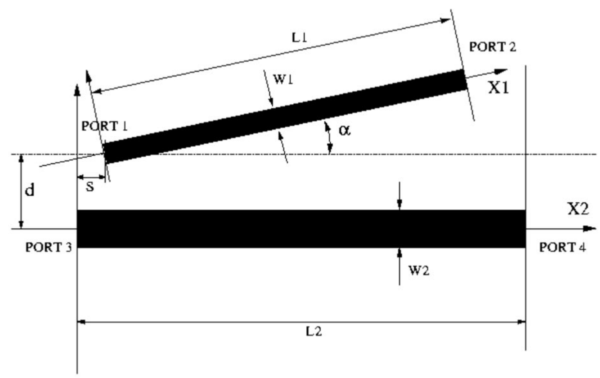

Fig. 1. Two coupled lines, composing a four-port.

I. INTRODUCTION

COUPLING between lines in microwave circuits can become large, especially when the lines are close to each other and run parallel. In order to solve a circuit correctly, this coupling should be taken into account. A classical way to do this is to use a subsectional method of moments. The whole circuit is divided into segments that are small compared to the wavelength. The current is then expanded into basis functions that represent the current between two adjacent segments. In the next step, the fields that a current of a basis function generates at all positions between two adjacent segments are calculated. A set of equations can now be written which expresses that, for every position between two adjacent segments, the total tangential electric field on the conductors has to be zero (impedance boundary condition). The current on the conductors is calculated by solving these equations. From this current the coupling (in decibels) can be calculated. The advantage of this method is that it can handle random shapes, by meshing them into squares and triangles. In the case of lines, however, it does not take advantage of certain physical relations for transmission lines that are known in advance. As a result the matrix may become very large for more complicated circuits and the solution will take a lot of computer resources. By taking into account these known physical relationships, the coupling between lines can be calculated a lot faster. Fig. 1 shows the structure that is used to explain the method. Two lines are located in a multilayered structure (e.g., microstrip, stripline, etc.). The technique explained further in this paper can handle arbitrary directions of both lines, as long as they are sufficiently separated. Both lines have ports at both ends. All ports are terminated in the characteristic impedance of the corresponding line. The objective is to calculate the 4 × 4 S-matrix, which represents the coupling between the four ports. It is essential to understand that only the coupling between lines 1 and 2 is calculated. The coupling between the structures feeding the lines is not considered. The reason for this is that the technique presented here will be used as a module in an overall approach for the analysis of planar structures, where the coupling from and to the feeding parts is taken into account in a different way.

In this paper, the results of the developed method are compared with those of a standard method of moments. The theory and corresponding software that implements this standard method are described in [1]–[3]. Other methods to solve this problem are discussed in [4]–[6].

Manuscript received May 3, 1999. This work was supported by the Flemish Institute for the Advancement of Scientific-Technological Research in Industry under a scholarship.

The authors are with the Department of Elektrotechniek, Katholieke Universiteit Leuven, Heverlee B-3001, Belgium.

Publisher Item Identifier S 0018-9480(00)07398-1.

II. ITERATIVE SOLUTION FOR STANDARD METHOD OF MOMENTS

In this section, we will explain how, for a structure consisting of two lines, the equations expressing the impedance boundary condition for the two lines can be decoupled and solved iteratively.

In a standard method-of-moments procedure, the structure of Fig. 1 is solved as described in Section I. The resulting set of equations expressing the impedance boundary condition is shown in formula 1. The Nth column of the Z matrix describes the fields that the Nth current basisfunction generates at all basisfunction positions

$$\begin{bmatrix} Z_{11} & Z_{12} \\ Z_{21} & Z_{22} \end{bmatrix} \begin{bmatrix} I_{1e} \\ I_{2e} \end{bmatrix} = - \begin{bmatrix} E_1 \\ E_2 \end{bmatrix}. \quad (1)$$

The excitation [right-hand side of (1)] represents the opposite of the incident field on the lines. This field is generated by imposed currents at the ports. The Z matrix can be divided into the following submatrices:

1) Z_{11} describes the self-coupling of line 1;
2) Z_{12} and Z_{21} are identical due to reciprocity and represent the coupling between line 1 and 2;
3) Z_{22} represents the self-coupling of line 2.

The e subscript on the unknown currents indicates that the results are exact if the segmentation density goes to infinity. The relation between these imposed currents and the incident waves on the lines is determined in the deembedding step [7].

To solve (1) iteratively, we rewrite it as

$$\begin{aligned} I_{1e} &= -Z_{11}^{-1}E_1 - Z_{11}^{-1}Z_{12}I_{2e} \\ I_{2e} &= -Z_{22}^{-1}E_2 - Z_{22}^{-1}Z_{21}I_{1e}. \end{aligned} \tag{2}$$

When only port 1 is fed (indicated by the subscript $p1$), and we assume that this feed only produces a field on the first line ($E_{2p1} = 0$), then iterative approximations for I_2 and I_1 can be obtained as follows:

$$\begin{aligned} n &= 1, \qquad I_2^{(1)} = 0 \\ n &= 2, \qquad I_1^{(2)} = -Z_{11}^{-1}E_{1p1} \\ n &= 3, \qquad I_2^{(3)} = -Z_{22}^{-1}Z_{21}I_1^{(2)} \\ n &= 4, \qquad I_1^{(4)} = I_1^{(2)} - Z_{11}^{-1}Z_{12}I_2^{(3)} \\ &\vdots \end{aligned} \tag{3}$$

in which n is the number of the iteration step.

III. Basic Method

This section explains how the S-parameters are calculated, normalized to the line impedances.

Since the correction in each step of (3) is proportional to $Z_{12}^{(n-1)}$, sufficient accuracy will be reached rapidly if the norm of Z_{12} is small. A small value for the norm of Z_{12} indicates low coupling values between the two lines. Low coupling means that the lines are sufficiently separated. In this paper, it is further assumed that only line 1 is fed ($I_2^{(1)} = 0$). Also, only two iteration steps will be used. This means that we will only consider coupling from the "source" line (which is fed) to the "observation" line and ignore the influence of the induced observation line current on the source line (higher order coupling). If the coupling between the lines becomes too large, we can improve the results by using more iteration steps, which will take the higher order couplings into account again one by one. A general rule of thumb is: if the coupling is equal to $-x$ dB, then the second-order effect on the source line will be $-2x$ dB and on the observation line $-3x$ dB. This is also shown in Section V. The method cannot be used for tightly coupled (-5 dB or higher) lines because the β values of the lines change due to the development of odd and even modes.

Since coupling is low and the S-matrix is calculated with all lines terminated in their characteristic impedance at the ports, instead of being calculated using step 2 of (3), the current on line 1 may be approximated by a traveling wave. If a unity amplitude voltage wave excites line 1 at ports 1 or 2, then the current on line 1 can be approximated by

$$I(\text{line 1}) = \frac{e^{-j\beta x1}}{Z_{c1}} \quad \text{(Exited at port 1)} \tag{4a}$$

$$I(\text{line 1}) = \frac{e^{j\beta x1}}{Z_{c1}} \quad \text{(Exited at port 2).} \tag{4b}$$

Using step 3 of (3), we can now calculate an approximation for the current on line 2. Instead of the regular Z_{22} matrix, which describes the piece of line open at its both ends, we use a modified Z_{22m} matrix, which describes the same line, but matched at both ends (ports). This matrix will be derived in the following section. Thus, the Z-matrix used for line 2 is inherently matched. This means that, if port 3 is at $x = 0$ and port 4 is at $x = L2$ on line 2, the relationship between traveling voltage waves (needed for the calculation of the S-parameters) and the currents is simply

$$V_3^- = Z_{c2}I_2, \qquad x = 0 \tag{5a}$$

$$V_4^- = Z_{c2}I_2, \qquad x = L2. \tag{5b}$$

The subscripts on V denote the port number. The minus sign on V_3 and V_4 shows that these are the outgoing waves. The current at these points can only be due to outgoing waves because the ports are matched. Once we know the voltage waves at the ports, we can calculate S_{31} (V_3^-/V_1^+ with $V_1^+ = 1$) and S_{41} (V_4^-/V_1^+ with $V_1^+ = 1$) and from reciprocity we also know S_{13} and S_{14}. The S parameters will be symmetric provided that voltage and current waves are normalized: the current on the source line should be multiplied with the square root of the source line impedance and the outgoing wave on the observation line should be divided by the square root of the observation line impedance. By repeating the above with line 1 fed at port 2 (4b) instead of port 1 (4a), we can calculate S_{32}, S_{42}, S_{23}, and S_{24}. Although the S-parameters for the lines are calculated while they are terminated in their own characteristic impedance, these S-parameters can be easily renormalized to other impedances or used to calculate nonmatched cases. The remaining problem is how to express that line 2 is matched.

It is assumed that only one subdivision along the widths of the lines is used. This yields an excellent approximation as long as the coupled lines are far apart compared to their width. If more subdivisions along the widths are required, then the lines should be divided into parallel longitudinal current strips for which the same procedure can be used. The results for the different strips should be combined according to the current density profile across the width of the lines.

In the remainder of this paper, we will discard the iteration number subscripts. All currents are the result of the first two iterations.

IV. Derivation of Z_{22m} From Z_{22}

In this section, a method will be described that can be used to simulate a matched termination for a line. This matched termination is needed because we want the current at the ports to be equal to the outgoing current wave [(5a) and (5b)]. The quality of the match is not influenced by the position of the line or the

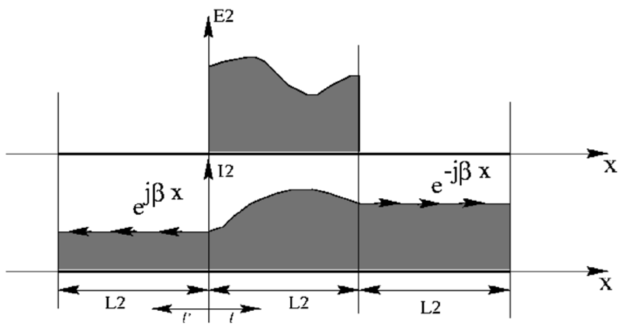

Fig. 2. Extension of the observation line at both ends.

vicinity of other lines. Subscript 2 is dropped for the coordinate system of line 2. The basis functions are counted in increasing x direction.

A method to match line 2 is derived from [4]. The first and last rows of Z_{22} are replaced by rows corresponding to

$$I_2(1)e^{j\beta\, dl} - I_2(2) = 0 \tag{6a}$$

and

$$-I_2(N-1) + e^{j\beta\, dl} I_2(N) = 0 \tag{6b}$$

respectively, where N is the number of basis functions on the line and dl is the segment length (half the length of a basis function). Equation (6a) states that at the left-hand-side termination of the observation line, there can only be a left-hand-side traveling wave and no right-hand-side traveling wave. Equation (6b) takes care of the termination at the right-hand side of the line.

The matching obtained using solely this technique is not perfect because of the sudden stop of the line at the terminations. Ideally, matching the line means prolonging it up to infinity at both sides and imposing traveling waves, going to infinity, on the prolonging pieces in such a way that the current is continuous at both ends of the line. This is explained in Fig. 2. We will approximate the infinite prolongations by reusing the proper Green's function to calculate coupling with a finite $(\text{length} = L2)$ virtual prolongation of the line. This Green's function was already calculated for this maximum distance $(L2)$ in the regular method-of-moments procedure because it was needed for the calculation of Z_{22}. Since this Green's function is known up to a distance corresponding to the length $(L2)$ of line 2, the field in a certain point x on the line can be approximated by

$$E_x(x) = \int_{x-L2}^{x+L2} \text{GF}(x-x')I(x')\, dx, \qquad 0 \le x \le L2. \tag{7}$$

The coupling from the virtual prolongation to the line can be calculated up to a distance equal to the length of the original line. Coupling across larger distances is neglected. The field generated by the virtual extension of the original line can be approximated by

$$E_x(l) = \int_{0}^{L2-l} \text{GF}(l+l')I(l')\, dl', \qquad 0 \le l \le L2 \tag{8}$$

in which l and l' are the distances from the port under consideration on the original line and the virtual extension, respectively. This is indicated for the left port in Fig. 2. The larger l becomes, the less accurate this approximation of the infinitely long line becomes because the integration interval (over the prolongation) becomes smaller and smaller. This can be tolerated because, at larger distances from the port, the coupling from the prolongation becomes negligible compared to the coupling of the line itself.

The following paragraph will explain how this theory can be implemented into the Z_{22} matrix to make the observation line appear matched.

The central piece of the prolonged line in Fig. 2 (from $x = 0$ to $x = L2$) is exposed to the incident field from the source line (upper graph). This field causes a current I_2 on the matched observation line, which is drawn in the bottom graph. The left-hand-side extension runs from $x = -L2$ to $x = 0$ and carries a current equal to

$$I_{\text{left}}(x) = I_2(0)e^{j\beta x}. \tag{9a}$$

The right-hand-side extension runs from $x = L2$ to $x = 2L2$ and carries a current equal to

$$I_{\text{right}}(x) = I_2(N+1)e^{-j\beta(x-L2)}. \tag{9b}$$

The current on the extension lines is fully known as a function of $I_2(0)$ and $I_2(N+1)$. This implies that the basis functions on the extension lines only yield two extra unknowns—namely, $I_2(0)$ and $I_2(N+1)$. Z_{22} is a Toeplitz matrix. Its first column contains the coupling factors between the basis functions of the observation line as a function of distance. This can be seen as a discrete Green's function on a basis function level. These coupling factors can also be used in the calculation of the coupling from the extension lines to the central piece: the basis function on the right-most side of the left-hand-side extension can be coupled to basis functions 1 through $(N-1)$ of the central line. Since we only know the coupling up to a distance of $(N-1)$ segment lengths, every next basis function of the left-hand-side extension (going right- to left-hand side) can be coupled to one basis function less of the central line. The faster the coupling decreases as a function of distance, the better this approximation becomes.

We can now construct a "matched" version of Z_{22}. We first add modified versions of (6a) and (6b) (two extra rows) as follows:

$$I_2(0)e^{j\beta\, dl} - I_2(1) = 0 \tag{10a}$$

$$-I_2(N) + e^{j\beta\, dl} I_2(N+1) = 0. \tag{10b}$$

These equations express the current continuity at the line to prolongation transition. N is the number of subsectional basis functions used in the original line.

We then calculate the couplings of $I_2(0)$ and $I_2(N+1)$ to the rest of the line. These will be put in two extra columns.

$$C(i) = \sum_{n=1}^{N-i} Z_{22}(i+n, 1) \cdot e^{j\beta\, dl(n-1)}, \qquad 1 \le i \le N-1 \tag{11}$$

where i denotes the index of the basis function on the center (original) line for which the coupling from the extension line is being calculated. The matched version Z_{22m} of the self-coupling matrix is then

$$Z_{22m} = \left[\begin{array}{c|ccc|c} e^{j\beta\, dl} & -1 & 0\ 0\ 0\dots & & \dots 0 \\ \hline C(1) & & & & 0 \\ C(2) & & & & C(N-1) \\ \cdot & & & & \cdot \\ \cdot & & & & \cdot \\ \cdot & & & & \cdot \\ & & Z_{22} & & \\ \cdot & & & & \cdot \\ \cdot & & & & \cdot \\ \cdot & & & & \cdot \\ C(N-1) & & & & C(2) \\ 0 & & & & C(1) \\ \hline 0\dots & & & \dots 0\ \ 0\ \ 0 & -1e^{j\beta\, dl} \end{array}\right]. \tag{12}$$

The matrix equation that expresses the impedance boundary condition for a matched line now becomes

$$Z_{22m}\begin{bmatrix} I_2(0) \\ I_2(1) \\ \vdots \\ I_2(N) \\ I_2(N+1) \end{bmatrix} = -\begin{bmatrix} 0 \\ E_2(1) \\ \vdots \\ E_2(N) \\ 0 \end{bmatrix}. \tag{13}$$

The quality of the matching at the ports can be checked by splitting the current into a left- and a right-hand-side traveling current wave using

$$\begin{bmatrix} I^+(x) \\ I^-(x) \end{bmatrix} = \begin{bmatrix} 1 & -1 \\ e^{-j\beta\, dx} & -e^{j\beta\, dx} \end{bmatrix}^{-1} \begin{bmatrix} I(x) \\ I(x+dx) \end{bmatrix}. \tag{14}$$

The splitting can be done in a discrete manner in terms of the current coefficients of the basis functions. The segment length is then used as dx. At a port, the splitting is calculated using the current at the port itself and the current calculated at one segment length away from the port, inside the line. Good matching means only outgoing waves at the ports. In Section V, this technique was used to check the quality of the matching (Fig. 3). The dependence of the reflection at the port on the length of the extension [the summation interval in formula (11)] is shown in Section V. It is clear that the reflections at the port become smaller as the used prolongation length increases. For normal usage, this extension length is always set to the maximum calculable distance, which is equal to the length of the line.

Once the Z_{22m} matrix for the matched observation line is known, the coupling between the two lines of Fig. 1 can now be obtained as follows. The current column matrix of line 1 (I_1) is calculated using (4a) or (4b). Multiplying Z_{21} with I_1 yields the incident field column matrix on line 2 (E_2). We can then get the current column matrix on the second (matched) line from

$$I_2 = Z_{22m}^{-1}(Z_{21} \cdot I_1). \tag{15}$$

It is important that there are no reflections because the S-parameters are calculated with the lines terminated in their characteristic impedance. If the matrix is not "matched," then the

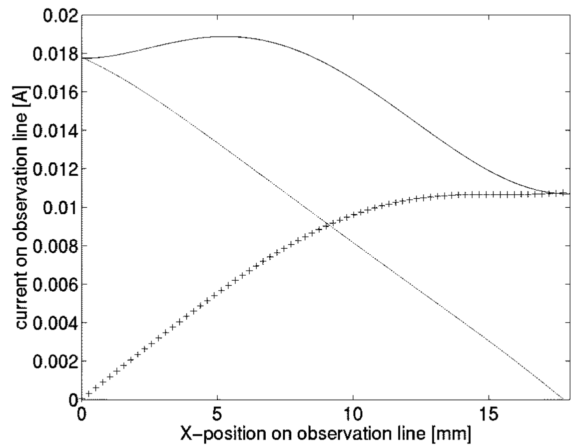

Fig. 3. Current on observation line: $-$ = left-hand-side traveling wave, $+$ = right-hand-side traveling wave, continuous line = total current.

calculated currents at the ends of the observation line will be zero (open) and the outgoing waves cannot be calculated. If $I1$ was calculated using (4a), then S_{31} and S_{41} can be calculated using

$$\begin{aligned} S_{31} &= -Z_{c2}I_2(0) \\ S_{41} &= Z_{c2}I_2(N+1). \end{aligned} \tag{16}$$

S_{32} and S_{42} are calculated in the same way, using (4b) to calculate I_1.

V. Numerical Results

The method described above is tested for the case of two parallel pieces of line. The substrate used has a thickness of 0.508 mm and a relative permittivity of 2.2. The distance d (Fig. 1) between the lines is equal to 4 mm. Both lines have a width of 1.542 mm (characteristic impedance of 50 Ω) and are 18-mm long. The results of the new method are calculated using only one segment along the width of the lines. The standard method of moments used in this section is described in [1]. For this standard method, five segments are used along the width of the lines. Both methods use 72 segments along the length of the lines.

First, the quality of the match obtained with the Z_{22m} matrix is examined at 5 GHz. This is done by splitting the current on the observation line into right- and left-hand-side traveling waves, for the source line port 2 excited. The result is shown in Fig. 3. The ratio between I^- and I^+ at the ports is approximately -60 dB, which proves the validity of the method.

Once the quality of the match is verified, we can use the new technique to calculate the S parameters and compare them to the S parameters obtained using the full standard method-of-moments procedure. The results are shown in Fig. 4.

There is an excellent agreement between the results of the two methods. This shows that, for this line–line distance, the current profile along the widths of the lines, which was not taken into account at all because only one segment along the widths was used, has only a minor effect on the mutual coupling. This also shows that second-order coupling is still negligible for this line–line distance.

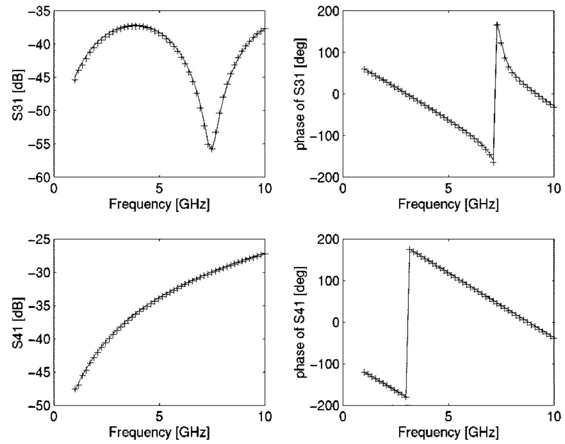

Fig. 4. Comparison of the S-parameters obtained by the standard method of moments (continuous line) and the new method (+ line).

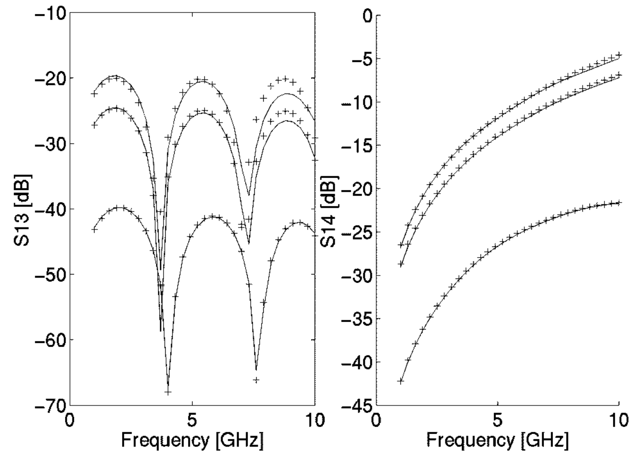

Fig. 6. Comparison for distances of 1 mm (top trace), 1.5 mm (middle trace), and 4 mm (lowest trace) for S_{13} (left-hand-side graph) and S_{14} (right-hand-side graph).

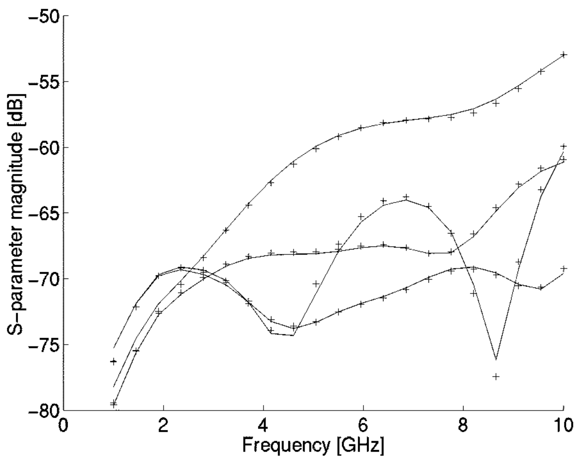

Fig. 5. Comparison of the S-parameters obtained by the standard method of moments (continuous line) and the new method (+ line).

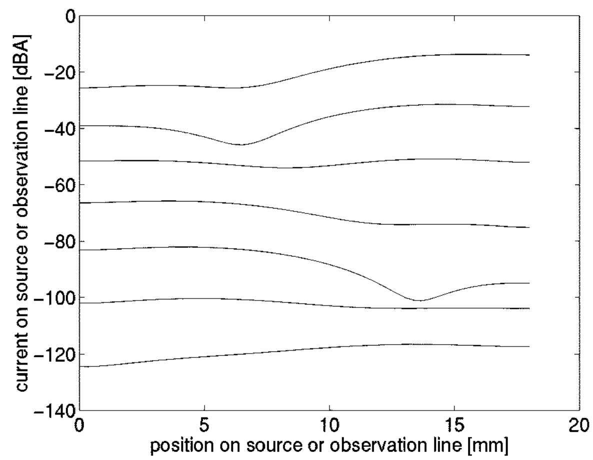

Fig. 7. Magnitude of the current on the line for first-order and higher order modes. The top curve is first order, the next curve is second order, etc.

This calculation was performed on a P-II 450-MHz machine running Linux. For the example given, the new method needed 0.0133 s per frequency point. The standard method needed 412.29 or 0.1499 s using five segments or one segment along the widths of the lines, respectively. These times include only inversion and deembedding. The matrix setup time is not included because this procedure was not changed.

Another example shows the validity of the method for general cases. Referring to Fig. 1, the dimensions are $d = -12.32$ mm, $S = 18.66$ mm, $\alpha = -60°$, $L1 = 40$ mm (31 segments), $W1 = 1.7$ mm (49 Ω), $L2 = 25$ mm (51 segments), $W2 =$ 1 mm (69 Ω). The substrate is the same as for the first example. The results for S_{13}, S_{14}, S_{23}, and S_{24} are shown in Fig. 5 and compared to the results of the standard method of moments.

To check the maximum allowable coupling level (minimum distance), another example was calculated consisting of two parallel lines $(\alpha = 0)$ with $S = 0$. Both lines have a length of 18 mm and a width of 0.61 mm (50 Ω). The substrate is 0.635-mm thick and $\varepsilon_r = 9.9$. The coupling was calculated and compared to the standard method of moments (using 80×5 segments for both lines) for the three distances of 4, 1.5, and 1 mm.

The continuous line in Fig. 6 represents the standard method of moments, the dotted–dashed line the new method. The results are usable up to 1.5 mm. The maximum coupling is then -10 dB (S_{14}). At closer distances (higher couplings), the results become bad at high frequencies and the curves shift in frequency because the β values start changing due to the coupling.

For the distance of 1.5 mm and a frequency of 5 GHz, Fig. 7 shows the magnitude of the first-order and higher order currents on the source and observation lines. The highest curve represents the first-order current on the observation line. The next trace shows the influence of this current on the source line, etc. The sum of all these currents (only the first ten orders are shown) will correspond to the solution obtained by full matrix inversion. From Fig. 7, it is clear that the higher order modes soon become negligible, which proves the fast convergence of the method and suggests that only one iteration step is sufficient in most cases.

The last example, shown in Fig. 8, illustrates the dependence of the reflection at the ports on the length of the virtual extension. A traveling wave incites on a matched termination and the reflected wave is calculated using (14). The continuous line is

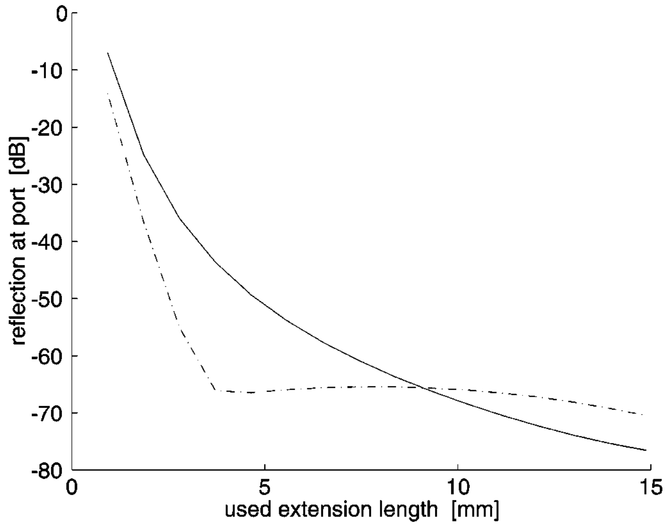

Fig. 8. Reflection at a port as a function of the length of the virtual extension. Continuous line has $\varepsilon_r = 2.2$, dashed–dotted line has $\varepsilon_r = 9.9$.

for a line length of 40 mm and width of 1.542 mm (50 Ω) on a substrate with a thickness of 0.508 mm and $\varepsilon_r = 2.2$. The dashed–dotted line is for a line length of 40 mm and width of 0.61 mm (50 Ω) on a substrate with a thickness of 0.635 mm and $\varepsilon_r = 9.9$. Both lines have 43 segments along the length and five segments along their width. The calculations where performed at 5 GHz. About one-tenth of a wavelength is needed to get good results. The left-most point of the curves corresponds to the technique that was used in [4], where no virtual prolongation was used.

VI. CONCLUSIONS

A new technique for the calculation of line–line coupling has been presented. It drastically reduces the calculation time: 1) by using the fundamental mode on the source line; 2) by using an inherently matched observation line; and 3) by neglecting higher order coupling. Using this technique, only the self-coupling matrix for line 2 (Z_{22}) and the coupling matrix between lines 1 and 2 (Z_{21}) have to be calculated. Only Z_{22} needs to be inverted instead of the complete line–line coupling matrix in a full method-of-moments procedure. Since the observation line is inherently matched, no deembedding step is needed.

REFERENCES

[1] G. A. E. Vandenbosch and A. R. Van de Capelle, "Mixed-potential integral expression formulation of the electric field in a stratified dielectric medium—Application to the case of a probe current source," *IEEE Trans. Antennas Propagat.*, vol. 40, pp. 806–817, July 1992.

[2] ——, "Accurate modeling tool for coaxially fed microstrip patch configurations in stratified dielectric media," *Arch. Electron. Uebertrag. Tech.*, vol. 49, no. 3, pp. 151–159, 1995.

[3] B. L. A. Van Thielen and G. A. E. Vandenbosch, "MAGMAS: Present status," in *Proc. COST 245 ESA Active Antennas Workshop*, Noordwijk, The Netherlands, June 1996, pp. 149–159.

[4] M. I. Aksun and R. Mittra, "Estimation of spurious radiation from microstrip etches using closed-form Green's functions," *IEEE Trans. Microwave Theory Tech.*, vol. 40, pp. 2063–2069, Nov. 1992.

[5] R. Gillard, J.-H. Corre, M. Drissi, and J. Citerne, "A general treatment of matched terminations using integral equations modeling and applications," *IEEE Trans. Microwave Theory Tech.*, vol. 42, pp. 2545–2553, Dec. 1994.

[6] E. K. L. Yeung, J. C. Beal, and Y. M. M. Antar, "Multilayer microstrip structure analysis with matched load simulation," *IEEE Trans. Microwave Theory Tech.*, vol. 43, pp. 143–149, Jan. 1995.

[7] J. Sercu, N. Fache, and D. De Zutter, "Characterization of TEM and non-TEM planar transmission lines with a full-wave 3D field analysis technique," in *Proc. 23rd European Microwave Conf.*, 1993, pp. 328–329.

[8] E. K. L. Yeung, J. C. Beal, and Y. M. M. Antar, "Matched load simulation for multiport microstrip structures," *Electron. Lett.*, vol. 29, no. 10, pp. 867–868, May 1993.

Bart Van Thielen was born in Belgium, on May 8, 1970. He received the M.S. degree in electrical engineering from the Katholieke Universiteit Leuven, Leuven, Belgium, in 1996.

He is currently a Research and Teaching Assistant with the Telecommunications and Microwaves Section, Katholieke Universiteit Leuven. His research interests are mainly in the area of electromagnetic theory, numerical methods, and electromagnetic compatibility.

Guy A. E. Vandenbosch (M'92) was born in Sint-Niklaas, Belgium, on May 4, 1962. He received the M.S. and Ph.D. degrees in electrical engineering from the Katholieke Universiteit Leuven, Leuven, Belgium, in 1985 and 1991, respectively.

From 1985 to 1991, he was a Research and Teaching Assistant with the Telecommunications and Microwaves Section, Katholieke Universiteit Leuven, where he was involved with modeling of microstrip antennas with the integral equation technique. From 1991 to 1993, he was a Post-Doctoral Researcher at the Katholieke Universiteit Leuven, and is currently a Professor. He is an active member of COST 260, a European project on "smart antenna computer design and technology." He has authored or co-authored papers appearing in international journals conferences. His research interests are mainly in the area of electromagnetic theory, computational electromagnetics, planar and conformal antennas, and electromagnetic compatibility.